Effect of Ethanolamine as Capping Agent on ZnS Nanoparticles: Structural Characterization and Photo Degradation of Toxic Dyes

Rohini. A. Khaparde[1], S. A. Acharya[2]

Department of Physics, RTM Nagpur University, Nagpur-440033, M.S., India

Abstract: *The high temperature wurtzite phase of ZnS was successfully obtained at low temperature (120°C) in the presence of ethynolamine (ENA) as the soft template. X-ray diffraction confirms the ENA-mediated phase transformation (zinc blende to wurtzite) of ZnS. UV-VIS spectra exhibits blue shift in all the samples. As the molar concentration of the capping agent increases, the absorption edge shifts to a lower wavelength. This blue shift of the absorption edges are evidence for different-sized ENA coated ZnS nanoparticles. In the present attempt, effects of phases and particle size of ZnS on photodegradation of dyes are systematically studied. Photodegradation of cango red, methylene blue, malachite green and dye waste collected from local industry, are systematically investigated by adding different molar proportional of ZnS in the dye. The rate of de-coloration of dye is detected by UV-VIS absorption spectroscopy. A significant reduction in the phase transition temperature and enhancement in photodegradation ability of ZnS has been achieved as compared to the bulk transition temperature (1020°C).*

Keywords: Nanoparticles, ZnS, Ethanolamine, photocatalysts, photodegradation, Malachite green.

1. Introduction

Synthesis of Colloidal semiconductor nanocrystals with controlled size, structure and morphology has received stimulated attention in the field of research because of their unique electronic, optical properties originating from quantum confinement effect and physical properties such as mechanical, thermal, magnetic, etc. which strongly depend upon the structure [1-4]. Therefore, in condensed matter physics or material science there is immense interest on the investigation of the effect of pressure and temperature on phase transformation. In nanoscale materials additional factors like interfacial energies or surfactants, solvents, templates, if any, and other experimental parameters also can influence the structural transformations due to aggregation and atomic motions at nanoscale[1, 5-6]. It is also possible to grow nanomaterials of desired structure on the seeds.

Semiconductor nanoparticles can be used in various applications like photocatalysis, imaging, solar cells, etc. with an increase in efficiency, just by manipulating its band gap energy which is the function of particle size [1,7-9]. Apart from the size control of nanocrystals, manipulating the shape and phase of nanocrystals, is also an important goal of modern material science, as it provides an opportunities to tune and explore nanocrystal's optical properties [1, 9−12]. Particularly, the differences in their crystalline structure and size can lead to considerable changes in the effective masses of electrons, holes, and energy gaps. The surface morphology also plays an important role in determining the properties of the system, especially at nanoscale due to their large surface-to-volume ratio. Photon Absorption is directly proportional to surface area-to-volume ratio. Because, large the surface-to-volume ratio, larger will be the number of surface trap states and so prolong is the photocarrier lifetime. Thus the active area of the charge carrier gets confined along with the shorten transit time, which plays a very important role in the photodegradation of toxic dyes.

So, in order to control the shape and phase of these nanostructures, surfactants play an essential role because of their soft-template effect, their ability to modify the chemical kinetics and simple maneuverability [1,12-24].

Among various semiconductors, ZnS, is one of the semiconductor having tremendous importance in the field of research and is being synthesized in various sizes and shapes so as to improve its performance and utilization in various applications from sensing devices to photonic material in molecular electronics and to advanced oxidation techniques [13, 25-27]. In addition to this, ZnS has been examined as a photocatalyst, due to its high energy conversion efficiency, the relatively negative redox potential of its conduction band carbon dioxide reduction and splitting for H_2 evolution [13,28-30]. And thus it is helpful to overcome the problem of water contamination due to toxic and most hazardous organic dyes and dyestuffs, resulted due to rapid population and industrialization specially from textile industries, which releases approximately, 50 to 70% of azo dyes and aromatic azo compounds which are highly carcinogenic along with their degradation products such as aromatic amines.[13,25,31]

ZnS exists in two crystalline forms, namely sphalerite (cubic phase) with a band gap of 3.66 eV and wurtzite (hexagonal phase) with a band gap of 3.77 eV at room temperature [1, 32-33]. Among these, the cubic structure of zinc sulfide is the most stable form in the bulk, which transforms into a thermodynamically metastable state called wurtzite structure at 1020 °C and melts at 1650 °C[1,9]. In both structures, Zn and S are tetrahedrally bonded with the only difference in the stacking sequence of atomic layers in cubic and hexagonal structures.[1] The properties of materials change dramatically with size, including thermodynamic stability. Also, structural transformations have been demonstrated to take place in nanoscale materials at lower temperatures [1, 34].

In the present attempt, we have tried to systematically investigate the effect of Ethanolamine on the structure and particle size of ZnS. Also we have tried to systematically study the effects of particle size on photodegradation of dyes are systematically studied.

2. Experimental

All chemical reagents were used as it is without any purification and procured from Merck. Double distilled water was used throughout to prepare the aqueous solutions. The salts of Zinc acetated [(Zn (CH$_3$COO)$_2$. 2H$_2$O) 98%], was used as source of metal ions. The sodium sulfide flakes (Na$_2$S.xH$_2$O) was used as precipitation reagent of metal ions. The Malachite Green stock solution with concentration of 0.5mgL^{-1} was prepared by dissolving Malachite Green oxalate powder (CAS.No.2437-29-8) in double distilled water.

0.1 mole Zinc acetate was added in 100 ml of solvent which is a mixture of (100-x)% of double distilled water and x% of Ethanolamine[NH$_2$CH$_2$CH$_2$OH]; and kept for constant stirring on hot plate with magnetic stirrer for 30 minutes at 60^0 C. We have taken x=20%, 50%, 70%, 90%, and 100% (to the total volume of solution, 100 mL) as a x:(100− x) volumetric ratio of ENA:H$_2$O. Then 0.1 ml of Na$_2$S is then added to get white solution. The resultant solution is stirred for 30 minutes at 60^0 C for homogeneus mixing. The solution was then transferred into a flask with reflexure and condenser and preceded at 120^{0}C for 24 h. The obtained solution was washed with water by centrifuging it for 15 minutes at 6000 rpm and precipitated is dried at 60^{0}C in hot air vacuum oven. The structure and phase purity of the sample was checked by X-ray powder diffraction (XRD) using Bruker AXS D8 Advance and PAN analytical X Pert Pro X-ray diffractometer equipped with copper target (λ_1, CuKα_1=1.5405 A^0). The data were collected with a step size of 0.05^0 and 0.016711^0 and step time of 2s and 5.08s respectively. Absorption spectra were obtained on a Perkin Elmer Lambda 35 Serial No. 502512621910 UV–vis spectrometer.

The photocatalytic degradation behavior of Malachite Green catalyzed with ZnS prepared by using different molar concentration of Ethanolamine was studied under UV-Vis irradiation. The absorption spectrum of Malachite Green sample at λmax of 617 nm was obtained on a Perkin Elmer Lambda 35 Serial No. 502512621910 UV–vis spectrometer. The decrease of absorbance value of the samples at λ$_{max}$ of dyes
(1) with the increase in the concentration of the samples
(2) The degradation efficiency was calculated as:

$$\%D = 100 \times [(C_o-C_t)/C_o] = 100 \times [(A_o-A_t)/A_o] \quad --- \quad (1)$$

where, C$_o$ and C$_t$ are the initial concentration and the concentration of dye in time of t, respectively, A$_o$ and A$_t$ are the initial absorbance and the absorbance of sample in time t, respectively and t is irradiation time of sample [25].

3. Results and Discussion

The XRD patterns of ENA capped ZnS with different molar percentage of ENA are shown in Fig 1a-e. For the sample with ENA=20%, the diffraction peaks are observed at 28.85°, 48.01°, and 57.45°. These peaks are identified due to (111), (220), and (311) planes of cubic or zinc blende structures of ZnS (JCPDS no 800020). The effect of ENA on the phase transition of ZnS is clearly evident from Figure 1. With an addition of ENA=50% into an aqueous solution, the XRD pattern shows the emergence of new additional peaks. For 50% EN, four new peaks are emerging out at 2θ = 27.49°, 31.09°, 40.28°, and 52.61° with three old peaks overlapping at 28.87°, 48.04°, and 56.74°. All the peaks are recognized with planes (100), (002), (101), (102), (110), (103), and (112) of the wurtzite phase of ZnS (JCPDS card no. 751534). All diffraction peaks of the sample are matched well to that of the wurtzite phase of ZnS crystal, indicating that the wurtzite phase has been formed in the sample in the presence of ENA.
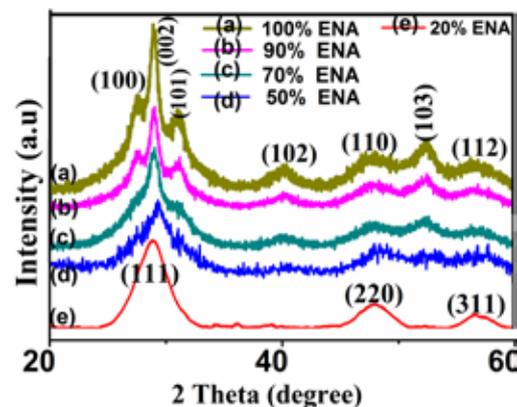
Figure 1: XRD Pattern of as synthesized ZnS

With increasing ENA concentration, the relative intensity (I(hkl)/I(002)) of the new peaks due to (100), (101), (102), and (103) planes is found to be increasing (see Fig 2). Generally, peak intensity is a measure of the total scattering from each plane and is directly dependent on the distribution of atoms in the structure. It reflects the degree of crystallinity of the particular plane. The trend of increasing relative intensity indicates that the degree of crystallinity of the wurtzite phase of the ZnS is becoming stronger with increasing ENA concentration. The crystallinity is also related to the concentration, reaction temperature, time, and the particle size measured. In the present work, there is high uniformity maintained in reaction conditions, while synthesizing all the samples, except a variation of ENA concentration in water. It implies that the variation in the degree of crystallinity observed here is only due to the different percentage of ENA used for sample preparation.
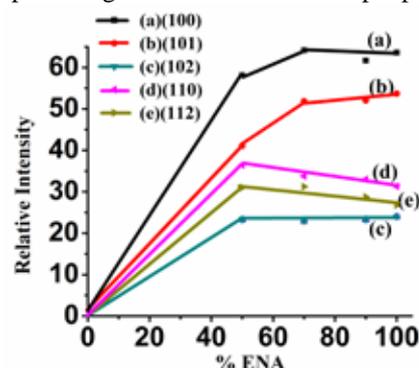
Figure 2: Increase of Relative Intensity of XRD peak with ENA concentration
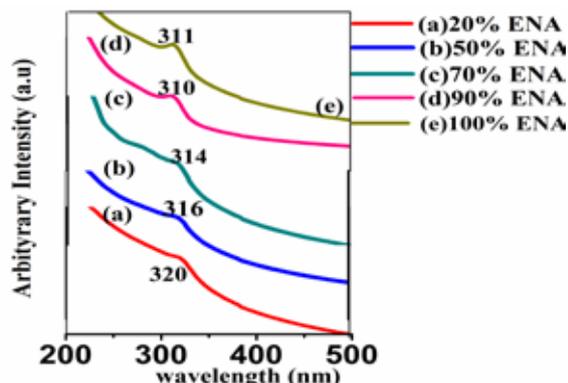
Figure 3: UV-Visible Spectra ZnS NPs with % of ENA (a) 20%, (b) 50%, (c) 70%, (d) 90% and (e) 100%

Fig 3 shows UV-VIS Spectrum of ZnS with increasing percentage of ethanolamine. The anamolies in absorption spectra are observed at 320 nm, 316 nm, 314 nm, 310 nm and 311 nm for ENA percentage of 20%, 50%, 70%, 90% and 100%, respectively. The blue shift of about 10 nm, 14 nm, 16 nm, 20 nm and 19 nm are observed as compared to bulk counterparts (E_g = 3.66eV for cubic and 3.77ev of wurtzite). This may contribute to the quantum confinement effect of photogenerated electron-hole pairs [35,36].The optical band gaps (E_g) is found to be 3.88 eV, 3.93 eV, 3.96 eV, 4.01 eV and 4.0 eV for ZnS with ENA percentage of 20%, 50%, 70%, 90% and 100% respectively. The particle size at these wavelengths, is calculated by the formula using the effective mass approximation model of Brus

$$E_g^* = E_g^{bulk} + \frac{\hbar^2 \pi^2}{2r^2}\left(\frac{1}{m_e^*} + \frac{1}{m_h^*}\right)$$

E_g is band gap energy of the nanoparticles which will be determined from UV-Vis absorption spectrum, E_g^{bulk} is band gap energy of the bulk ZnS at room temperature which has value of 3.66 eV for cubic and 3.77eV for Wurtzite, $\hbar$- is plank's constant, r- is particle radius, m_e is effective mass

of electron = 0.25 m_0 m_h is effective mass of hole = 0.59 m_0 and m_0 is free electronic mass = 9.11×10^{-31} Kg. The particle size at that particular wavelength is found to be 4.32 nm, 3.62 nm, 3.37 nm, 2.99 nm and 3.07 nm for ZnS with increasing percentage of ENA i.e. 20%, 50% 70% 90%, and 100% respectively. Thus we got a decreasing particle size with increasing percentage of ethanolamine.

The capping agent tunes the rate of chemical reaction which directly affects on evolution time of the number of nuclei. The nucleation and growth process is determined by this. When the chemical reaction is faster the nucleation becomes faster. The growth will be strongly influenced by number of nuclei present at given instant. Rate of nucleation drives autocatalytic growth, which leads to a large number of small particles. On other hand, autocatalytic growth is controlled by chemical reaction.

Table 1: Crystalline size and optical band gap of ZnS nanoparticles with different Percentage of capping agent

Percentage of Ethanolamine	Crystalline size (nm)	Optical band gap E_g (eV)
ENA=20%	4.32	3.8
ENA=50%	3.6	3.9
ENA=70%	3.4	3.9
ENA=90%	3.0	4.01
ENA=100%	3.1	4.0

Rate of reaction depends on the molar concentration of reactants solution and increases with the increase in molar concentration or Percentage of surfactant in reactants solution. In the present study, the percentage of capping agent varies from 20% to 100%, the reaction rate is highest for 90% and 100% which is approximately the same and hence the particle size obtained is smallest for the materials with these two percentage of surfactant as compared to other materials in the series, which is in consistent with the above made argument.

479

International Journal of Science and Research (IJSR)
ISSN (Online): 2319-7064, Impact Factor (2013): 4.438
www.ijsr.net
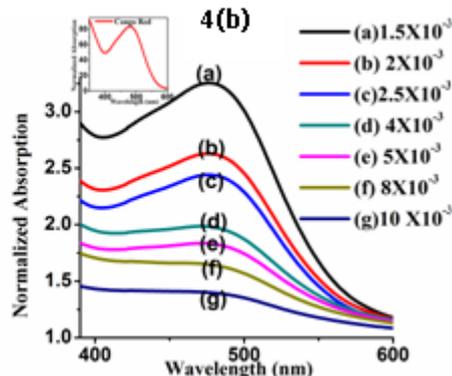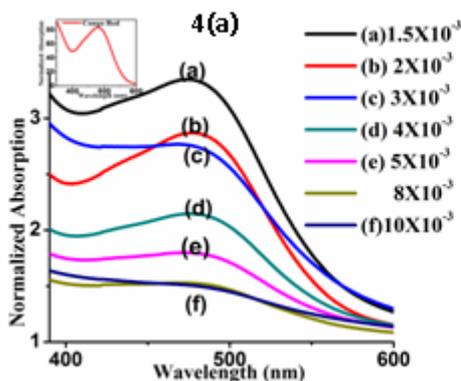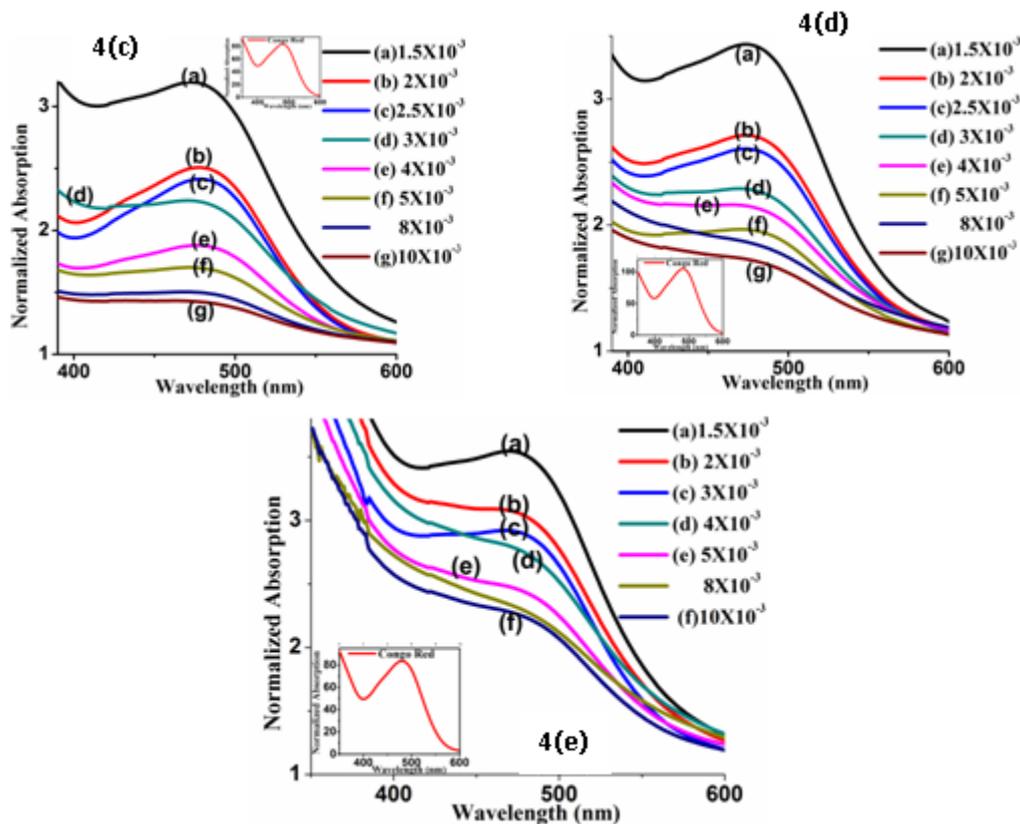
Figure 4: Photodegradation of Malachite Green (MG) by ZnS, synthesized with ENA percentage of 20% (4a), 50% (4b), 70% (4c), 90 % (4d) and 100% (4e)

To investigate the potential applicability of the as-synthesized ZnS nanoparticles, the photocatalytic degradation of Malachite Green (MG) was examined in the presence of the ZnS (synthesized with different % of ENA) under UV-irradiation. The characteristics absorption of MG at 617 nm was chosen respectively as monitored parameter for the photodegradation process. The stock solutions of dyes are prepared on basis of their VIS-absorption intensity. Thus optimized stock solution of MG are obtained as 2 mgL^{-1} water, The absorption spectrum of the aqueous solution of MG in presence of ZnS (synthesized with different % of ENA) in different molar proportion (from 1 to 10 mmolL^{-1}) under UV-VIS light irradiation are displayed in Fig 4a, 4b, 4c, 4d and 4e for ENA percentage of 20%, 50%, 70%, 90% and 100% respectively. From the figure, we can see that the absorption peaks corresponding to the MG (at 617 nm) diminishes gradually as the molar concentration of ZnS increases for each sample. Furthermore, we can see that there is no new absorption band appears in the either visible or ultraviolet regions, which indicates the complete photodegradation of MG, without newly formed species. The same is repeated for other dyes also like Congro Red, Methylene Blue and Waste as collected from local industry. Almost same trends of photodegradation are observed.
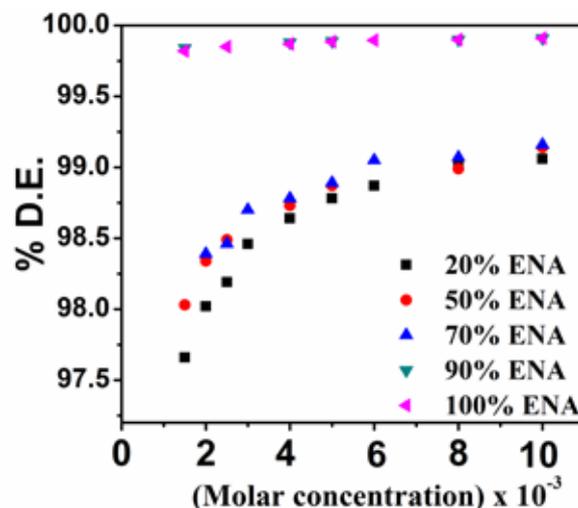
Figure 5: Percentage degradation efficiency of MG by ZnS NPs with different percentage of ENA

Degradation efficiency (D.E.) is calculated by using equation (1). The comparative degradation efficiency for MG at different molar concentration of all ZnS samples indicates that ZnS with 90% and 100% ENA is relatively more capable to degradate dyes than ZnS other percentage of ENA as shown in fig 5.

This is obvious as the Photodegradation of toxic dyes is surface phenomena. Surface characteristics play an important role in the adsorption of reactants and desorption of products. Photon Absorption is directly proportional to surface area-to-volume ratio. Because, large the surface-to-volume ratio, larger will be the number of surface trap states and so prolong is the photocarrier lifetime. Thus the active

area of the charge carrier gets confined along with the shorten transit time. For nano-scale semiconductor particles this ratio is much greater than their bulk counterparts, and thus allows greater photon absorption on the photocatalyst surface. Moreover, with the decrease in particle size, volume recombination (radiation less recombination) of the electron-hole pair within the semiconductor is also drastically reduced. For nanometer-size scaled semiconductor, the band-gap energy increases with the decrease in possibility of volume recombination which in turn led to higher redox potentials in the system. Therefore, the nano-scale semiconductor is expected to have higher photocatalytic activity than its bulk. In our case ZnS with 90% and 100% ENA has smallest particle size and largest band gap among all the others with complete wurtzite phase. These results clearly indicate that phase and size directly affects on photodegradation ability of ZnS.

4. Conclusion

In Summary, it is possible to produce different size of ZnS Nanoparticles using simple chemical method by using different percentage of capping agent. ZnS nanoparticles of 2 to 5 nm size are synthesized by co-precipitation route. ENA as a capping agent induces phase transformation from zinc blende to wurtzite with increasing molar concentration. The blue shift in UV-Vis absorption spectra of as-synthesized ZnS nanoparticles results from Quantum confinement effects. The potential of as-synthesized samples are investigated by studying photodegradation of Malachite green by adding different molar proportional of ZnS in the dye; until to get complete de-coloration of dyes. The rate of de-coloration of dye is detected by UV-VIS absorption spectroscopy. Very small concentration in range of mg/L proportion is needed for complete photodegradation of the dyes as compared bulk counterpart 10^{-2} g/L. The reduced particles size with the increase in surface area, is found to be affecting photoelectron /hole separation efficiency and hence rate of photodegradation. Phase and size of ZnS directly affect on photodegradation ability of ZnS.

5. Acknowledgement

References

[1] S. A. Acharya, Neeraj Maheshwari, Laxman Tatikondewar, Anjali Kshirsagar, and S. K. Kulkarni, Cryst. Growth Des. 13(2013)1369.
[2] Y. Zou, D. Li, and D.Yang, Nanoscale Research Letters 6(2011)374.
[3] P. Kumar, N. Saxena, R.Chandra, V.Gupta, A. Agarwal and D.Kanjilal, Nanoscale Research Letters 7(2012)584.
[4] S.B.Qadri, E.F. Skelton, D.Hsu, A.D. Dinsmore, J.Yang, H.F.Gray and B.R.Ratna, Physical Review B. 60(1999)9191.
[5] H. Zhang; J. F. Banfield, Nano Lett. 4(2004)713.
[6] H. Zhang; J. F. Banfield, Am. Mineral. 85 (1999) 528.
[7] A. P. Alivisatos, Science 271(1996) 933.
[8] M. Pal, N. R. Mathews, P. Santiago, X. Mathew, J Nanopart 14 Res (2012) 916.
[9] G.O. Siqueira, T. Matencio, H. V. da Silva, Y. G. de Souza, J. D. Ardisson, G.M. de Limaa and A.O. Porto, Phys.Chem. Chem. Phys., 15(2013) 6796.
[10] Wang, J.; Luo, H.; Chen, T.; Yuan, Z. Nanotechnology 2010, 21, 505603.
[11] Y. Zou, D. Li and D.Yang, Nanoscale Research Letters 6(2011) 374.
[12] K.D. Nisha, M. Navaneethan, Y. Hayakawa, S. Ponnusamy, C. Muthamizhchelvan, Materials Chemistry and Physics 136 (2012) 1038.
[13] J Li, Y. Xu, Y. Liu, D. Wu, Y. Sun, China Particuology. 2 (2004) 266.
[14] H. Fujiwara, H. Hosokawa, K. Murakoshi, Y. Wada, S.Yanagida, Langmuir 14 (1998) 5154.
[15] A. Henglein,. M. Gutierrez, Ber. Bunsen-Ges. Phys. Chem.87(1983) 852.
[16] J. M.Nedeljkovc, M. T.Nenadovi, D. I.Micic, A. Nozik, J. Phys.Chem. 90 (1986) 12.
[17] I.Spanhel, M.Haase, H.Weller, A. Henglein, J. Am. Chem. Soc. 109 (1987) 5649.
[18] M.Anpo, S.Kodama, Y. Kubokawa, J. Phys. Chem. 91(1987) 4305.
[19] D. W.Bahnemann, C.Kormann, M. R. Hoffmann, J. Phys. Chem. 91(1987) 3789.
[20] S.Yanagida, Y.Ishimaru, Y.Miyake, T.Shiragami, C.Pac, K.Hashimoto, T. Sakata, J. Phys. Chem. 92(1988) 3476.
[21] T.Shiragami, C.Pac, S. J. Yanagida, Chem. Soc., Chem.Commun. (1989) 831.
[22] T.Shiragami, C.Pac, S. J. Yanagida, Phys. Chem. 94(1990)504.
[23] L.Hu , J.Yan , M. Liao , H. Xiang , X. Gong , L. Zhang ,and X. Fang Adv. Mater., 24 (2012) 2305.
[24] S. Liu , J. F. Ye , Y. Cao , Q. Shen , Z. F. Liu , L. M. Qi , X. F. Guo , Small, 5 (2009) 2371.
[25] H.R. Pouretedal, M.H. Keshavarz, International Journal of the Physical Sciences. 6(2011) 6268.
[26] S. Senthilkumaar, R. Thamiz Selvi, N. G. Subramaniam, T. W. Kang, Superlattices and Microstructures 51 (2012) 73.
[27] S. Gupta, J.S. Meclure, V.P. Singh, Thin Solid Films 33 (1997) 299.
[28] X. Fang, L. Wu , and L. Hu Adv. Mater.23(2011) 585.
[29] J.-S. Hu, L.-L. Ren, Y.-G. Guo, H.-P. Liang, A.-M. Cao, L.-J. Wan, C.L.Bai, Angew. Chem. Int. Ed.44 (2005)1269.
[30] Q. Zhao, Y. Xie, Z. Zhang, X. Bai, Cryst. Growth Des. 7(2007) 153.
[31] G Liu, T. Wu, J. Zhao, H. Hidaka, N. Serpone. Environ. Sci. Technol. 33 (1999) 2081.
[32] X. S. Fang , Y. Bando , M. Y. Liao , U. K. Gautam , C. Y. Zhi , B. Dierr, B. D. Liu , T. Y. Zhai , T. Sekiguchi , Y. Koide D. Golberg , Adv. Mater. 21 (2009) 2034 .
[33] H.C. Ong, R.P.H. Chang, Appl. Phys. Lett. 79 (2001) 3612.
[34] C. S. Tiwary, C. Srivastava, P. Kumbhakar, J. Appl. Phys. 110 (2011) 34908.
[35] Y. Chen, R.Yin, Q. Wu, J. Nnaomaterials 2012 (2012) 6.
[36] P. Calandra, M. Goffredi, V.T. Liveri, J.Colloids and Surfaces 160 (1999) 9.